Review Article

3D-printed stretchable conductive polymer composites with nano-carbon fillers for multifunctional applications

Chenpeng Zhao†, Ruqing Li†, Biao Fang, Rui Wang, Han Liang, Lei Wang, Ruilin Wu, Yunan Wei, Zhangyuan Wang, Zhipeng Su, Runwei Mo*

School of Mechanical and Power Engineering, East China University of Science and Technology, Shanghai 200231, China

*** Corresponding author:** Runwei Mo, rwmo@ecust.edu.cn

† Chenpeng Zhao and Ruqing Li contributed equally.

Abstract: Carbon nanomaterials are widely used as substrate materials to prepare stretchable conductive composites due to their good stability, strong conductivity, and low price. In response to the demand for optimizing the performance of composite materials, various manufacturing methods for preparing carbon nanomaterial-reinforced stretchable conductive composite materials have emerged. Among them, 3D printing technology has the advantages of flexible processes and excellent product performance and has received widespread attention. This review focuses on the research progress of adding carbon nanomaterials as reinforcing phases to polymer materials using 3D printing technology. The application prospects of conductive polymer composites based on nanocarbon fillers in aerospace, energy storage, biomedicine, and other fields are prospected.

Keywords: carbon-based materials; 3D printing technology; polymer composites; structural design; electronic devices

1. Introduction

A stretchable conductive composite material prepared based on a nano-carbon filler refers to a composite material that uses carbon material as a conductive filler. The key to stretchable conductive composites is the need to maintain the conductive network under large strains and recover its original properties after the strain is released. In general, flexible and elastic polymers have excellent stretch properties but poor electrical conductivity[1–4]. While carbon nanomaterials such as graphene, carbon nanotubes (CNT), and carbon black (CB) have high electrical conductivity[5], they have poor stretch properties[6,7]. Therefore, nano-conductive materials and stretchable polymers are usually mixed in a specific way to prepare stretchable conductive nanocomposites, which are applied to stretchable batteries, strain sensors, stretchable supercapacitors, and wearable medical device fields[8,9]. It is worth noting that, compared with metal conductive fillers, carbon materials have better stability and modification ability, a lighter weight, and a lower price, which makes large-scale production possible for meeting the growing demand for new electronic devices[10–18].

In recent years, 3D printing technology has developed very rapidly and has been widely used in many fields, such as aerospace, biomedicine, and energy storage[19–26]. It is considered to be a promising new manufacturing molding technology[27]. 3D printing technology also provides new ideas for the preparation of polymer-based composite materials[28,29]. Combining 3D printing technology with the preparation of carbon nanomaterials/polymer-based composite materials can achieve rapid manufacturing of composite materials[30–32]. This provides a new path for the manufacture of products with complex structures. The addition of carbon nanomaterials makes 3D printing products have better mechanical properties, electrical properties, and functional characteristics, and it is also more convenient to prepare gradient functional products[33,34]. In

Received: 7 November 2023 Accepted: 20 November 2023 Available online: 24 November 2023

addition, the layer-by-layer manufacturing method of 3D printing inhibits the large-area agglomeration of carbon nanomaterials in the polymer matrix, which is more conducive to achieving uniform dispersion[35]. As shown in **Figure 1**, the 3D-printed stretchable conductive polymer composites with nano-carbon fillers exhibit good mechanical and electrical properties, showing great application potential in the fields of electronics, aerospace, energy storage, and biomedicine. In this review, the research on the formation of carbon nanomaterials/polymer matrix composites by 3D printing is introduced, the preparation methods of carbon nanomaterials/polymer matrix composites are briefly introduced, and the 3D printing process and application fields are summarized.

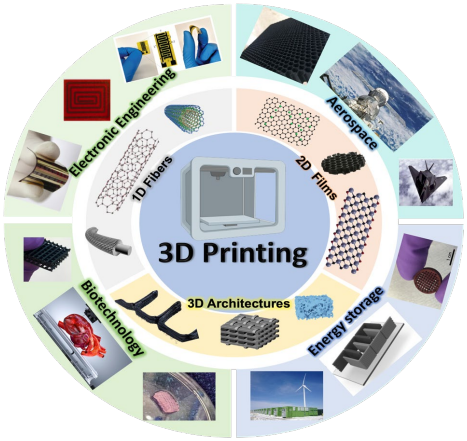

Figure 1. Scheme of 3D-printed stretchable conductive polymer composites with nano-carbon fillers and their applications.

2. Classification of carbon-based polymer composites

Carbon materials are currently one of the most widely used materials due to their advantages, such as low price, good stability, abundant raw material reserves, and good biocompatibility[36]. It mainly includes graphite, carbon fiber, carbon black, graphene, graphyne, carbon nanotube, and fullerene (C_{60}). Graphite is the most common carbon material and is often used in corrosion-resistant materials, lubricating materials, refractory materials, and raw materials for preparing graphene oxide[37]. Carbon fiber is a special fiber mainly composed of carbon elements[38]. It has excellent mechanical strength and modulus along the fiber axis. Therefore, it is often used as a reinforcing material to combine with polymers, metals, or ceramics to prepare composite materials. C_{60} is a new type of hollow molecule composed entirely of carbon. At present, it is mostly used as an electron-transport layer in the field of organic solar cells, which can improve the photoelectric conversion efficiency of the cells[39]. However, carbon black, graphene, and carbon nanotubes have smaller sizes and excellent electrical properties and belong to nanoscale conductive materials. Therefore, it is widely used in stretchable conductive nanocomposites.

2.1. Carbon black

As one of the most important carbon-based fillers, carbon black has been widely used in various industrial productions. This nanomaterial has a series of advantages, such as a high specific surface area, good chemical stability, high electrical and thermal conductivity, and low cost. Carbon black is mainly produced by the thermal decomposition or incomplete combustion of hydrocarbon compounds. The size, structure, and conductivity of carbon black particles are largely determined by the choice of raw material and method of manufacture. Carbon black particles have an amorphous and quasi-graphite structure, and the average particle size of carbon black is 3–100 nm. It is worth noting that carbon black particles tend to agglomerate together to form aggregates, and these aggregates will form larger spatial network structure aggregates under the action of the van der Waals force. Therefore, avoiding the agglomeration of carbon black particles is the focus and

difficulty of research. Recently, Bhagavatheswaran et al.[40] successfully prepared a composite material by mixing carbon black and styrene-butadiene rubber, as shown in **Figure 2(a–c)**. It is worth noting that the researchers prevented the agglomeration of carbon black by adding silica particles. The results showed that the composite had an electrical conductivity of 40 $S.m^{-1}$ and a maximum stretch of 200%, and its application in pressure sensors was explored. Niu et al.[41] successfully prepared a stretchable conductive composite using carbon black and polydimethylsiloxane, as shown in **Figure 2(d–f)**. The research results showed that the composite material had good electrical conductivity and mechanical stability, which can be used to assemble biological microchips. Song et al.[42] used carbon black and carbon nanotubes mixed with polybutylene adipate/terephthalate (PBAT) to prepare a composite material, which was used as a current collector in aqueous lithium-ion batteries, as shown in **Figure 2(g–i)**. The research results showed that it still worked normally under 100% strain, and the electrical conductivity of the composite material significantly improved after adding carbon nanotubes.

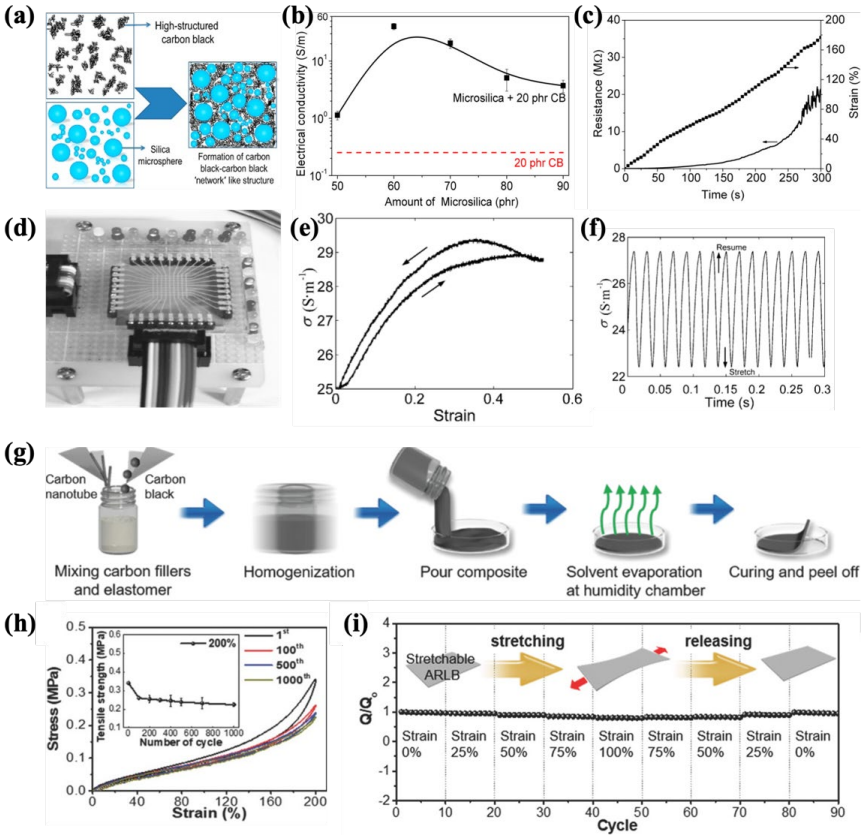

Figure 2. (a) Development of strong filler-filler network of conducting carbon black particle. **(b)** Plot of electrical resistance for hybrid composites with different microsilica contents. **(c)** Resistance with strain[40]. **(d)** Testing circuit with LEDs to show functionality of bonded plate. **(e)** Quasi-static stretching and restoring at rate of 1.5 $mm.min^{-1}$ for carbon black powder and PDMS (CPDMS). **(f)** Dynamic stretching characteristics of CPDMS sample, with peak-to-peak amplitude of 1 mm, 50 Hz[41]. **(g)** Steps for fabrication of carbon/polymer composite. **(h)** Fatigue test of stretchable electrode containing hybrid carbon/polymer composite under strain of 200% repeated for 1000 cycles. The inset shows the tensile strength of the electrode as a function of the number of strain cycles, with the maximum value being 1000 cycles. **(i)** Relative discharge capacity of stretchable aqueous rechargeable lithium-ion battery under various amounts of strain[42].

2.2. Carbon nanotube

From the analysis of crystal structure, a carbon nanotube is a hollow cylindrical tubular structure formed by curling graphene sheets (hexagonal structure) according to a specific helical angle. There are two types of carbon nanotubes: (1) single-walled carbon nanotubes (SWCNTs), which can be viewed as individual graphene sheets rolled into cylinders, and (2) multi-walled carbon nanotubes (MWCNTs), which can be

viewed as stacks of multiple concentric layers of graphene. There are many methods for preparing carbon nanotubes, mainly including laser ablation, arc evaporation, chemical vapor deposition (CVD), etc. Carbon nanotubes are ideal materials for the preparation of composite materials due to their high modulus, high stiffness, high electrical conductivity, and low density. Recently, Shin et al.[43] prepared a composite using MWCNTs obtained by chemical vapor deposition mixed with polyurethane. It is worth noting that almost no decrease in electrical conductivity of the composite was observed within a strain of 10%–20%, as shown in **Figure 3(a,b)**. Sekitani et al.[44] prepared a composite material by mixing single-walled carbon nanotubes and fluorinated rubber, as shown in **Figure 3(c–e)**. The as-prepared composite possessed an electrical conductivity greater than 100 $S.cm^{-1}$ and stretchability exceeding 100%. A stretchable active-matrix display was successfully constructed based on this composite. Liu et al.[45] used reduced graphene oxide (rGO) and carbon nanotubes as conductive fillers and styrene-butadiene rubber as a polymer to prepare a composite material, as shown in **Figure 3(f,g)**. The results of the study showed that the electrical conductivity of the composite reached 3.62 $S.cm^{-1}$ and was stable under low tensile strain. More importantly, compared with those of carbon black conductive nanocomposites, the performance of the composite significantly improved.

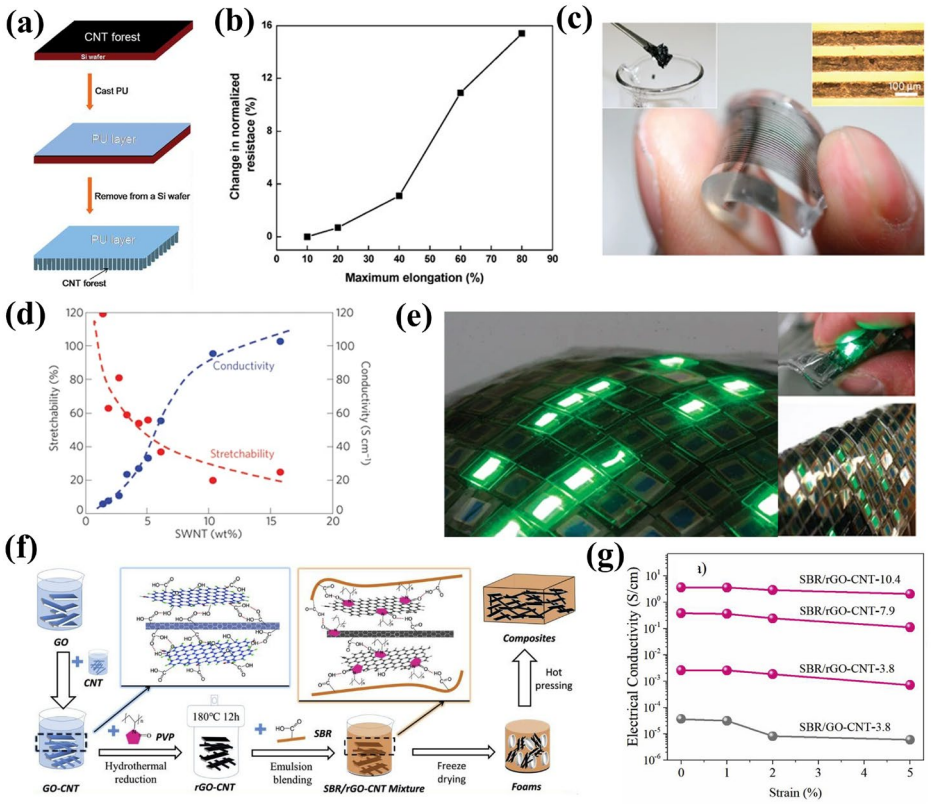

Figure 3. (a) Schematic diagram of preparation method for forest/polyurethane composite sheet. **(b)** Change in normalized resistance shown in graph in going from 10th to 100th cycle as a function of maximum applied strain. The first 10 cycles for each strain set were used to provide initial sample conditioning[43]. **(c)** Printed elastic conductors on PDMS sheet. **(d)** Stretchability and conductivity as function of SWCNT content. **(e)** Demonstration of stretchable display that can be spread over arbitrary curved surfaces. The stretchable display is functional even when folded in two or crumpled, indicating excellent durability[44]. **(f)** Schematic illustration for preparation of rGO-CNT hybrid and styrene-butadiene rubber (SBR)/rGO-CNT composites. **(g)** Changes in electrical conductivity of SBR/GO-CNT and SBR/rGO-CNT composites under different strains[45].

2.3. Graphene

Graphene consists of a single layer of carbon atoms arranged in a two-dimensional honeycomb lattice, which can be deformed to obtain other carbon materials. Graphene has many excellent properties, such as a high specific surface area, high electrical conductivity and electron mobility, excellent thermal and chemical

stability, and mechanical flexibility[46]. In addition, graphene can obtain a variety of derivatives through the method of interface modification. For example, element-doped graphene is the basis for constructing self-supporting graphene composites, which endow the composites with excellent mechanical, electrical, and thermal properties. Recently, Chen et al.[47] prepared graphene with a 3D structure by chemical vapor deposition, which was filled with polydimethylsiloxane to prepare a composite material, as shown in **Figure 4(a–c)**. The composite material exhibited excellent electrical conductivity, making it useful as a stretchable conductor in various fields. Wang et al.[48] prepared a stretchable graphene honeycomb composite structure using graphene foam and polydimethylsiloxane, as shown in **Figure 4(d–g)**. The composite had a conductivity of 72 $S.m^{-1}$. It is worth noting that a stretchable light-emitting display was successfully fabricated using this material as a circuit. In addition, Sun et al.[49] prepared stretchable conductive fibers using graphene and polyurethane fibers, which can be used for strain sensors and stretchable conductors, as shown in **Figure 4(h–k)**. However, the process of percolating 3D-structured graphene with polymers is usually complicated, which is not conducive to large-scale preparation.

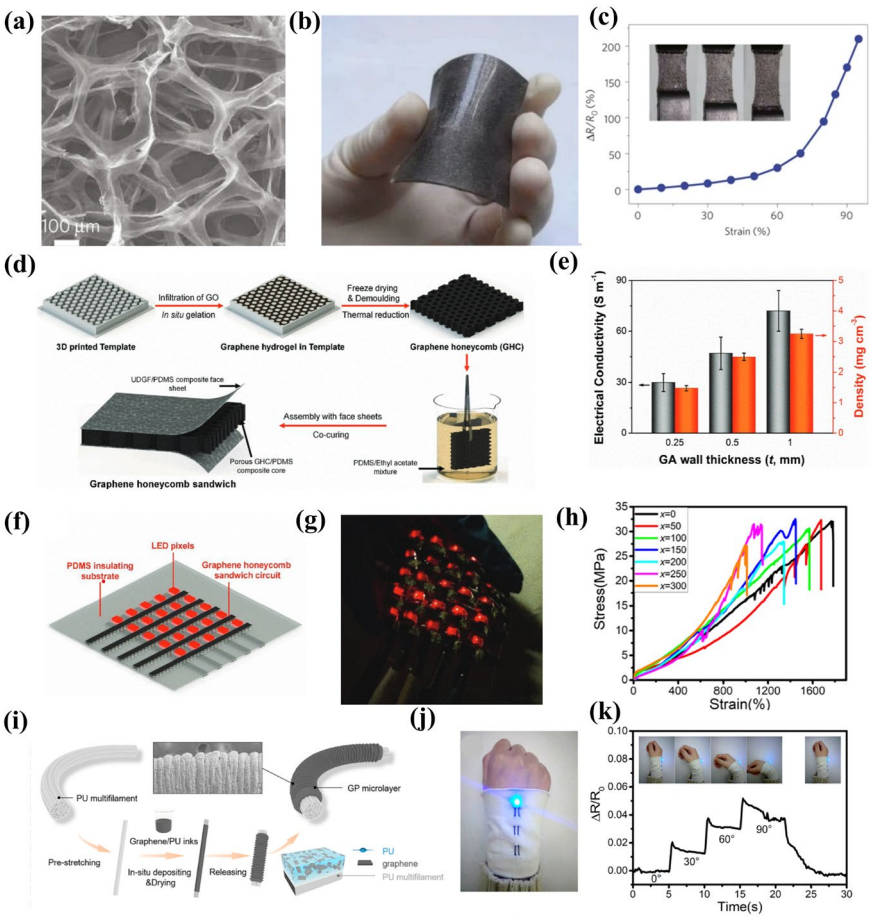

Figure 4. (a) SEM image of graphene foam (GF). **(b)** Photograph of bent GF/PDMS composite, showing its good flexibility. **(c)** Electrical conductivity of GFs and GF/PDMS composites as function of number of graphene layers[47]. **(d)** Fabrication of GHCs and GHC sandwiches. **(e)** Graphene honeycomb (GHC) with *t* ranging from 0.25 to 1 mm. **(f)** Schematic of stretchable light-emitting display constructed using GHC sandwich. **(g)** Photograph of stretchable light-emitting display[48]. **(h)** Conductivity-strain curves. **(i)** Schematic diagram of preparing worm-shaped filaments. **(j)** Potential applications of strain-insensitive stretchy electronics. **(k)** Filament woven into fabric to conduct signals under wrist joint movements[49].

In recent years, researchers have improved the performance of stretchable conductive composites by adding carbon nanomaterials. However, there are still some issues that need to be addressed. The most crucial aspect is achieving a uniform dispersion of carbon nanomaterials in polymer matrices. It is worth noting that the dispersion degree of carbon nanomaterials in polymers greatly affects the comprehensive performance of

composite materials. Therefore, in order to fully utilize the excellent mechanical and electrical properties of carbon nanomaterials, it is necessary to develop new mechanisms, methods, and technologies to achieve a uniform dispersion of carbon nanomaterials in polymers.

3. 3D printing process of carbon-based polymer composites

With the continuous development and improvement of 3D printing technology, various new 3D printing technologies have emerged endlessly. In recent years, the preparation of carbon-based polymer composites by 3D printing technology has developed rapidly[50]. At present, the 3D printing processes applicable to carbon-based polymer composites mainly include fused deposition modeling, inkjet printing, stereolithography apparatus, and selective laser sintering. Different printing processes have corresponding advantages and disadvantages, which need to be selected comprehensively according to the characteristics of printing materials, process characteristics, and product uses.

3.1. Fused deposition modeling

Fused deposition modeling (FDM) is mainly suitable for the 3D printing of thermoplastic polymers and is currently the most commonly used 3D printing method. Specifically, this method requires the polymer to be prepared into a standard-diameter wire, and then the wire is transported to the nozzle by a stepping motor, heated, and melted for extrusion. Finally, the layers are stacked and bonded according to the desired shape on the substrate, and the desired molding is obtained after cooling and solidification[51,52]. The fused deposition molding of the carbon-based polymer-based composite material can be performed by making the carbon-based polymer composite material via melt mixing, solution mixing, etc. into a 3D printing wire. The addition of nano-carbon materials can not only enhance the mechanical properties of composite materials but also endow composite materials with excellent electrical, thermal, friction, and wear properties.

It is worth noting that acrylonitrile-butadiene-styrene copolymers (ABS) and polylactic acid (PLA) are the most commonly used polymers for FDM. Recently, Wei et al.[53] prepared rGO/ABS and rGO/PLA composites by mixing polymers with graphene oxide (GO) via solution mixing and adding hydrazine hydrate for reduction, which were used for fused deposition molding after wire drawing, as shown in **Figure 5(a–d)**. The research results showed that the maximum amount of GO added reached 5.6% (mass fraction, the same as below) and electrical conductivity reached 1.05×10^{-3} $S.m^{-1}$. The addition of carbon nanomaterials increased the glass transition temperature (T_g) of the polymer, and so the 3D printing temperature needs to be increased appropriately compared with pure resin. Zhu et al.[54] mixed 6% graphene nanoplatelets (GNPs) with nylon 12 (PA12) for fused deposition molding, as shown in **Figure 5(e–j)**. The results showed that the GNPs were oriented during extrusion from the nozzle, which increased the thermal conductivity and elastic modulus of the composite along the direction of orientation by 51.4% and 7%, respectively, compared with those of compression molding. Fused deposition modeling not only has the advantages of a wide range of printing materials, easy operation, low equipment cost, easy operation, and fast printing speed, but it can also print different types of materials at the same time with multiple nozzles. Therefore, it is one of the most promising printing methods for industrial applications. However, this method also has shortcomings, including insufficient printing accuracy, blocked nozzles, uneven thermal stress, and low interlayer strength.

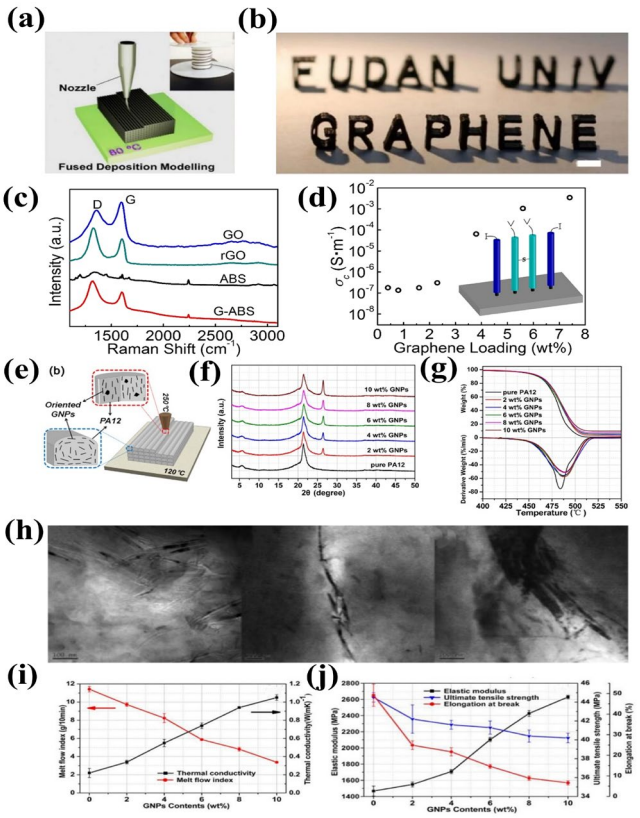

Figure 5. (a) Schematic illustration of fused deposition modeling in 3D printing process. Inset is graphene-based filament winding on a roller. The filament was deposited through a nozzle onto a heated building plate, whose temperature was set at 80 °C. **(b)** Typical 3D-printed model using 3.8wt% G-ABS composite filament (scale bar: 1 cm). **(c)** Representative Raman spectra in prepared GO, rGO, ABS and G-ABS samples. **(d)** Electrical conductivity (σ_c) of G-ABS composites as function of graphene loading. Inset is four-probe schematic setup used in σ_c measurement[53]. **(e)** Orientation of GNPs in PA12 matrix during FDM process. **(f)** XRD spectra of PA12 and PA12/GNP nanocomposites with 2, 4, 6, 8, and 10 wt% of GNP compression-molded samples (10 mm × 10 mm × 4 mm). **(g)** TG (top) and DTG (bottom) curves of pure PA12 and PA12/GNP nanocomposites with 2, 4, 6, 8, and 10 wt% of GNPs. **(h)** TEM micrographs of 6wt% PA12/GNP nanocomposite. **(i)** MFI values, thermal conductivity (λ). **(j)** Tensile test results of pure PA12 and PA12/GNP nanocomposites and their CM specimens[54].

3.2. Inkjet printing

Inkjet printing (inkjet) was developed from a technology that was originally only used for text and picture printing into a rapid prototyping method. As an additive manufacturing technology, it has been widely used in electronic circuits, flexible devices, etc.[55]. In the commonly used piezoelectric inkjet printing process, the printing material is first dissolved or dispersed in a solvent to form "ink". Then, according to printing needs, voltage is applied to the piezoelectric ceramic sheet to deform it, and the ink in the cavity is squeezed to be ejected drop by drop and accumulated layer by layer on the substrate to form the shape to be printed. Finally, the solvent setting is removed by heat treatment, freeze drying, and other post-processing methods[56]. The high carrier mobility of carbon nanomaterials makes them very suitable for restoring the electrical conductivity of nanoelectronic devices, making flexible materials with excellent electrical conductivity and dielectric properties. Inkjet printing is a commonly used, convenient, and efficient preparation method. The addition of polymers can stabilize the ink, prevent carbon nanomaterials from precipitation and stratification, and also adjust the viscosity of the ink for a range that is convenient for printing. It is worth noting that in order to adjust the viscosity of the ink, researchers found that polyvinylpyrrolidone (PVP) and ethyl cellulose (EC) could be added to the ink as stabilizers and viscosity regulators.

Recently, Lim et al.[57] dissolved GO and polyvinyl alcohol (PVA) in water, mixed them, and then reduced them with hydrazine hydrate to prepare an rGO/PVA ink, as shown in **Figure 6(a–g)**. Finally, the electrodes

of organic field-effect transistors were prepared by inkjet printing. The results showed that the field-effect mobility of the rGO/PVA electrode printed by inkjet printing greatly improved compared with the traditional Au and PEDOT:PSS electrodes. García-Tuñon et al.[58] grafted polymers on graphene oxide sheets to prepare pH-responsive surfactants. The research results showed that the viscosity of the obtained ink can be adjusted by changing the pH and finally, the continuous printing of three-dimensional molded objects can be realized through a 100μm nozzle, as shown in **Figure 6(h–j)**. Inkjet printing has the advantages of simple equipment, easy operation, and low cost. Therefore, it is very suitable for preparing micro-nano devices and electronic circuits. However, this method also has some defects, including the low strength of the prepared device, some defects after post-processing, and the device falling off the substrate.

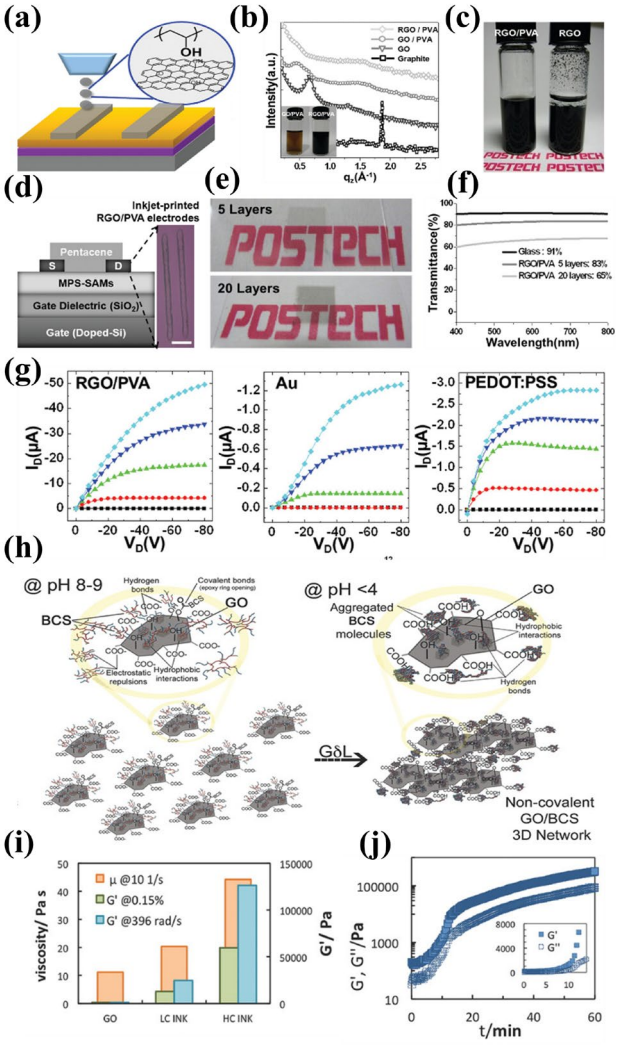

Figure 6. (a) Inkjet-printed rGO/PVA electrodes. **(b)** XRD patterns of graphite, graphite oxide (GO), GO/PVA, and rGO/PVA composite. Insert shows photographs of well-dispersed GO/PVA (left) and rGO/PVA (right) suspensions. **(c)** rGO/PVA composite stably dispersed in mixed solvent with DMF and water for three months (left) and rGO precipitated from same medium (right). **(d)** Schematic illustration of device structure. Insert is optical microscope image of inkjet-printed rGO-PVA composite electrodes (scale bar: 300 μm). **(e)** Photographs of rGO/PVA films with 5 and 20 layers fabricated by inkjet printing. **(f)** UV-Vis spectra of rGO/PVA films with 5 and 20 layers fabricated by inkjet printing. Transmittance was measured at λ = 550 nm. **(g)** Output characteristics of organic field-effect transistors based on different electrodes: Au (left), rGO/PVA (center), and PEDOT:PSS (right)[57]. **(h)** Sketch of directed assembly mechanism. **(i)** Histogram showing comparison of viscosity and storage modulus (G') of GO suspension (1.75 wt%) without additives (left), GO/branched copolymer surfactant (BCS) suspension with low graphene oxide concentration (1.75wt%, LC, middle), and highly concentrated GO/BCS ink (2.5wt% GO, HC, right). Viscosity at shear rate of 10 s^{-1} increased from 10 to nearly 50 Pa.s. **(j)** Kinetics of self-assembly followed by time sweep at fixed strain (1%) and frequency (0.1 Hz)[58].

3.3. Stereolithography apparatus

Stereolithography apparatus (SLA) is a molding method that uses photosensitive resin as the printing material. Specifically, a laser beam scans the surface of the liquid photosensitive resin according to the designed route to solidify a specific area of the photosensitive resin, thereby forming a cross-section of the model. Subsequently, the lifting table is moved down a small distance to solidify a new layer of section until a complete part is formed. Photosensitive resins generally include polymer monomers or prepolymers, photoinitiators, and other components[59]. The more commonly used types of photosensitive resins include unsaturated polyesters, epoxy acrylates, polyurethane acrylates, etc. When stereolithography apparatus is used to form carbon nanomaterials/polymer-based composites, carbon nanomaterials are generally dissolved in a solvent and then added to a photosensitive resin or directly added to the resin for mixing, followed by photocuring[60].

In recent years, Zhou et al.[61] added GO to a phosphate-buffered saline solution (PBS) of polyethylene glycol diacrylate (PEGDA) and gelatin methacrylate (GelMA) and then added a photoinitiator to form a photosensitive resin, as shown in **Figure 7**. GelMA and PEGDA are two commonly used photocurable biomaterials. It is worth noting that the addition of GO can promote the adhesion and growth of biological stem cells and induce stem cell differentiation. The research results showed that the photosensitive resin can be used for photocuring to prepare biological scaffolds and promote the differentiation of human bone marrow mesenchymal stem cells to form cartilage tissue. In addition, there are some reports of adding carbon nanomaterials directly to commercial photosensitive resins for printing to improve their mechanical properties. And the polymer can also be removed by high-temperature post-treatment, followed by thermal reduction of GO to prepare a three-dimensional rGO structure. Stereolithography apparatus has become one of the mainstream technologies in the current 3D printing market due to its high printing accuracy, excellent surface quality, and ability to form complex structures. However, the current bottleneck of this technology is mainly the high cost and the toxicity of the residual photoinitiator and uncured photosensitive resin. In addition, it is necessary to prevent carbon nanomaterials from settling out of the photosensitive resin during printing, resulting in an uneven distribution of carbon nanomaterials in the composite.

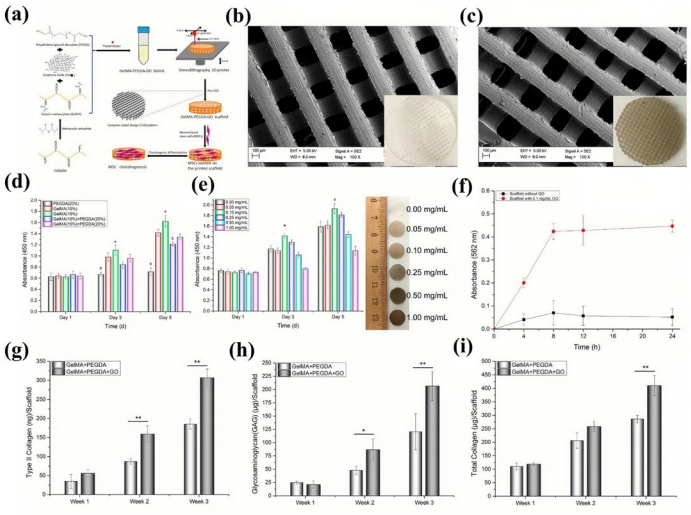

Figure 7. (a) Schematic diagram of 3D-printed GO scaffold for promoting chondrogenic differentiation of human bone marrow mesenchymal stem cells (hMSCs). **(b)** and **(c)** SEM micrographs of GelMA-PEGDA scaffolds without GO and with GO (0.1 mg/mL). **(d)** Mesenchymal stem cell (MSC) proliferation on hydrogels with different compositions for 5 d. **(e)** MSC proliferation on GelMA-PEGDA scaffolds incorporated with different concentrations of GO for 5 d. **(f)** Adsorption profiles of bovine serum albumin (BSA) on GelMA-PEGDA scaffolds with and without GO (0.1 mg/mL) at different time points. **(g)** Collagen II, (**h**) glycosaminoglycan (GAG), and **(i)** total collagen secretion of MSCs after chondrogenic differentiation on GelMA-PEGDA scaffolds without and with GO over three weeks[61].

3.4. Selective laser sintering

Selective laser sintering (SLS) is a 3D printing method suitable for powder molding, mainly used for printing metal and ceramic powders, and it can also be used for thermoplastic polymer powders[62]. During the printing process, the barrel first rises a certain distance and the powder spreading roller moves to spread a layer of powder material on the working platform[63,64]. Then, a laser beam is emitted by the laser, and the powder in the selected area is fused and sintered according to the cross-sectional profile under computer control so that the layers are increased. Gaikwad et al.[65] first melted and mixed carbon nanomaterials and nylon 11 (PA11) with a twin-screw extruder to granulate them, and then pulverized them at low temperature to form powders for selective laser sintering, as shown in **Figure 8(c–e)**. The research results showed that the addition of carbon nanomaterials not only improved the flexural modulus, Young's modulus, and thermal stability of nylon 11 but also made nylon 11 exhibit electrical conductivity, which can be used for static dissipation. Compared with other molding methods, the composite material obtained by selective laser sintering has better conductivity, and the amount of carbon nanomaterial required for electrostatic charge dissipation is small. In addition, carbon nanomaterials can enhance thermal conductivity, making the laser melting and sintering processes easier.

In addition, Shuai et al.[66] first synthesized GO/PVA composite powder by the solution mixing method and then prepared biological scaffolds by selective laser sintering, as shown in **Figure 8(a,b,f–h)**. Due to the strong hydrogen bond interaction between GO and PVA, the two were closely combined. The research results showed that the compressive strength, Young's modulus, and tensile strength of the scaffold added with 2.5% GO/PVA increased by 60%, 152%, and 69%, respectively, compared with those of pure resin. The advantages of selective laser sintering are that there is a wide range of moldable materials, different types of powder materials can be mixed and sintered to form composite materials, no support structure is required, and the material utilization rate is high. At present, there are relatively few reports on the formation of carbon nanomaterials/polymer matrix composites by selective laser sintering. The reported research works mainly focused on nylon-based materials, and future research can be extended to more types of composite materials.

In recent years, researchers have made significant progress in the preparation of carbon-based polymer composites through 3D printing. However, there are still some issues that need to be addressed. Problems, such as clogging nozzles and insufficient bonding force, are likely to occur during the 3D printing process, which greatly affect the performance of carbon-based polymer composites. In addition, there are currently relatively limited types of polymers that can be used for 3D printing, which requires further expansion.

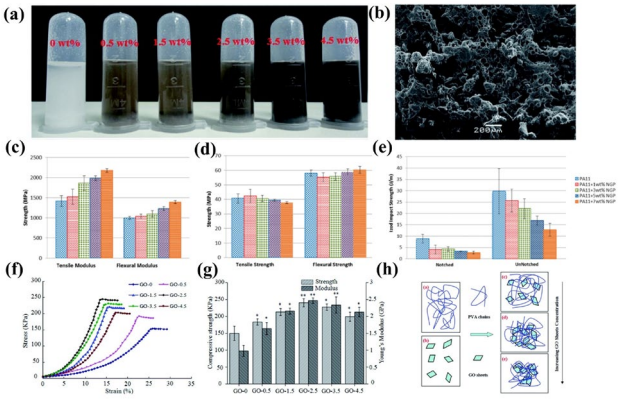

Figure 8. (a) Photographs of GO/PVA suspension with different GO loadings after ultrasonic dispersion. **(b)** Surface morphologies of scaffolds with different GO loadings of 2.5 wt%. **(c)** Tensile strength and flexural strength and **(d)** tensile modulus and flexure modulus of PA11 and PA11/ nanographene platelet (NGP) nanocomposites. **(e)** Izod impact strengths[65]. **(f)** Compressive properties of GO-0, GO-0.5, GO-1.5, GO-2.5, GO-3.5, and GO-4.5 stress-strain curves. **(g)** Compressive strength and Young's modulus of GO-0, GO-0.5, GO-1.5, GO-2.5, GO-3.5, and GO-4.5. **(h)** Schematic representation of PVA chains (inset: **(I)** GO sheets, **(II)** GO sheet dispersion in PVA matrix with various GO loadings, **(III)** 0.5 wt%, **(IV)** 2.5 wt%, and **(V)** 4.5 wt%)[66].

4. Applications of carbon-based polymer composites

4.1. Electronic field

As we all know, carbon nanomaterials have a large specific surface area and high carrier mobility, which makes them have great application potential in the field of electronics[67–71]. After compounding with a suitable polymer matrix, carbon nanomaterials can be used to prepare flexible electronic devices[72,73]. The application of 3D printing can conveniently and quickly form complex and exquisite electronic devices and can quickly integrate electronic components[74,75]. It is worth noting that one of the hot spots of graphene research in the field of electronics is the use of graphene in field-effect transistors (FETs). The higher carrier mobility of graphene makes a transistor made of graphene have a faster response speed, which can significantly increase the cut-off frequency of the transistor. In addition, due to the small thickness of graphene, the characteristic size of transistors can be reduced, and Moore's law can be further continued[76], which is an important research direction in the field of integrated circuits in the future.

The 3D printing method used to prepare graphene FETs is mainly inkjet printing. Recently, Xiang et al.[77] deposited graphene on a Kapton flexible substrate by inkjet printing and used ionic liquid/copolymer gel as the gate dielectric layer to prepare FETs, as shown in **Figure 9(a–c)**. Light-emitting diodes are optoelectronic devices that play an important role in communication, display, lighting, and other fields. Graphene has good transparent and conductive properties and can be used as an electrode material for light-emitting diodes. Researchers have also prepared graphene in a hydrogel state for inkjet printing[78]. In addition, electronic circuits prepared by 3D printing methods, such as inkjet printing and fused deposition modeling, can be used to connect various electronic devices, as shown in **Figure 9(d–h)**.

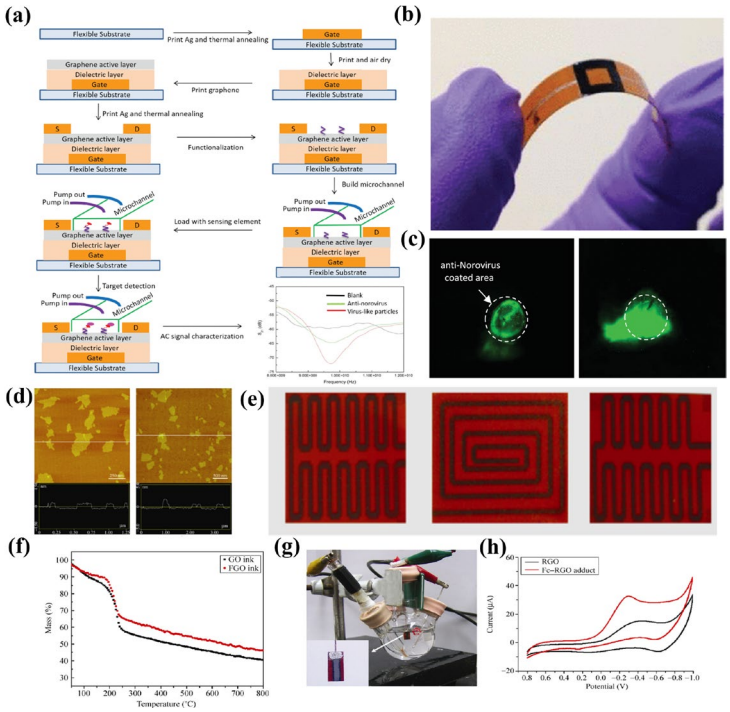

Figure 9. (a) General fabrication procedures and signal output of graphene FET biosensor. **(b)** Graphene FET biosensor. **(c)** Epifluorescence staining with fluorescent-tagged secondary antibody identifies areas of printed graphene successfully coated with a target-specific Norovirus capture antibody. Dotted white circles indicate approximate area of primary antibody deposition[77]. **(d)** Typical tapping mode AFM images (top) and corresponding height cross-sectional profiles (bottom) of GO sheets in GO ink (0.1 mg/mL) and few-layered graphene oxide (FGO) sheets in FGO ink (0.1 mg/mL) deposited on mica substrate. **(e)** Patterns printed on polyimide using FGO ink with concentration of 5 mg/mL. **(f)** TGA curves of graphene oxide materials used in GO ink and FGO ink at heating rate of 10 °C in N_2 atmosphere. **(g)** CV measurements of H_2O_2 sensors. Three-electrode method was used to detect H_2O_2 in 0.05mol/L phosphate buffer solution (PBS) (pH 7.4) and 0.1mol/L KCl. Shown in the inset is a bare-printed graphene electrode. **(h)**

Cyclic voltammograms of rGO (black) and Fc-rGO adducts (Fc and reduced graphene oxide hybrid adducts) (red) modified printed graphene electrodes in 5mmol/L H_2O_2, 0.05mol/L PBS (pH 7.4), and 0.1mol/L KCl saturated with Ar at 50mV/s scan rate[78].

4.2. Aerospace field

In the field of aerospace, carbon-based polymer composites also show considerable application potential[79]. Due to the excellent mechanical properties of carbon nanomaterials, adding them to polymer matrices may significantly improve mechanical properties, such as tensile strength and elastic modulus[80–82]. It is well known that bismaleimide, epoxy resin, and phenolic resin are commonly used resin matrices in the aerospace field[83]. It is worth noting that after adding a small amount of carbon nanotubes, graphene oxide, or modified graphene to these resins, the mechanical properties significantly improved. In addition to being used to improve mechanical properties, carbon nanomaterials can also be used as functional reinforcements. Carbon nanomaterials can form a conductive network in a polymer matrix to improve the conductivity of the composite material and can be used for static dissipative materials and lightning strike protection for aircraft[84]. The addition of carbon nanomaterials to a polymer matrix can also enhance the thermal stability of the composite material, increase the carbon residue rate, and be used for the ablation of heat-resistant materials, as shown in **Figure 10(a–c)**. In addition, carbon-based polymer composites can be used for microwave absorption and electromagnetic shielding and are used in the field of aircraft stealth[85]. Due to the excellent performance of carbon nanomaterials in terms of mechanical properties and functionality, carbon-based polymer composites can also be used as structural/functional integrated materials in future aircraft, as shown in **Figure 10(d–g)**. The characteristics of 3D printing for rapid and precise forming of complex components, combined with the excellent functional properties of carbon-based polymer composites, will have great application potential in non-load-bearing parts of aircraft.

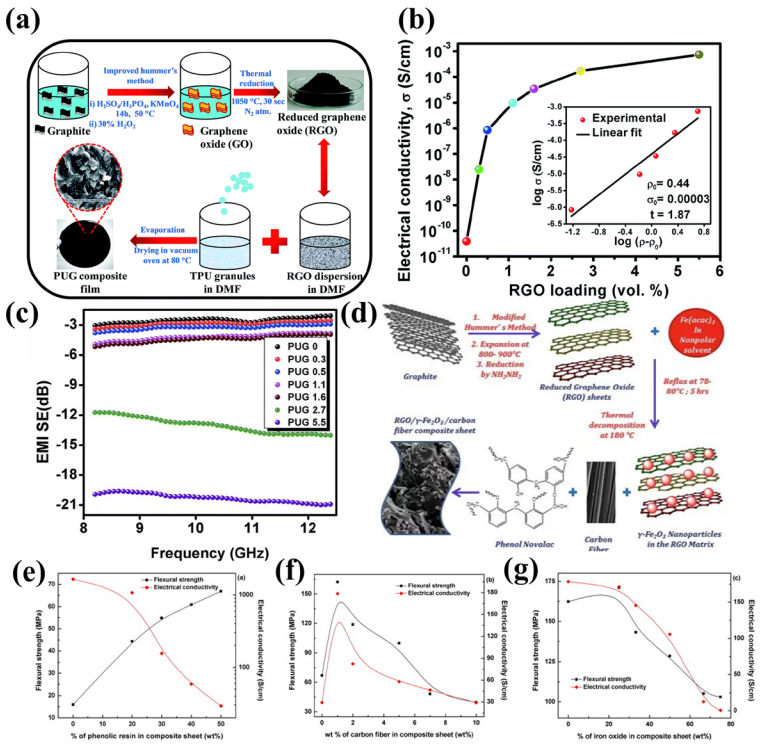

Figure 10. (a) Schematic representation of fabrication process of polyurethane graphene nanocomposite films. **(b)** Variation in electrical conductivity with rGO loading in thermoplastic polyurethanes (TPU) matrix. The inset shows the log(σ) vs. log(ρ − ρ0) plot. **(c)** Variation in EMI shielding effectiveness with frequency for polyurethane/graphene (PUG) nanocomposites[84]. **(d)** Schematic representation of preparation of phenolic resin-based composite sheets containing different wt% of rGO, γ-Fe_2O_3 nanoparticles and carbon fibers in organic medium. Variation of flexural strength and electrical conductivity as function of wt% of **(e)** phenol resin, **(f)** carbon fiber, and **(g)** γ-Fe_2O_3 in rGO sheets[85].

4.3. Energy storage field

Based on the excellent electrical conductivity and low thermal expansion coefficient of carbon nanomaterials, researchers have mixed carbon nanomaterials with anode or cathode active materials to form 3D lithium-ion batteries or used thermally responsive inks to mix carbon nanomaterials and Cu powder to form supercapacitors. In-depth research has been done on the potential application of high conductivity and low resistance properties of composite materials added with carbon nanomaterials in lithium-ion batteries and supercapacitors. Recently, Fu et al.[86] put water-based ink into a syringe and extruded filaments to print them layer by layer to prepare electrodes, as shown in **Figure 11(b–g)**. Then, the solidified electrode was freeze-dried and thermally annealed to obtain rGO. Lithium iron phosphate (LFP)/rGO and lithium titanium oxide (LTO)/rGO electrodes were prepared by the above 3D printing methods. Through the study of electrochemical performance, it was found that when rGO was added, the two Li-ion batteries almost reached the theoretical capacity of LFP and LTO at a specific current density of 10 mA/g. Among them, the initial charge-discharge capacity of LTO/rGO was slightly higher than the theoretical capacity of LTO. After the 10th and 20th cycles of cycling, the charge-discharge curves of the two electrodes were close to stable, and LTO/rGO maintained low voltage hysteresis.

Rocha et al.[87] used chemically modified graphene, a water-based thermal response formula mixed with Cu powder, and Pluronic F127 (thermal response ink) as reaction raw materials to prepare rGO/Cu electrodes with interlocking interfaces through 3D printing and heat treatment methods, as shown in **Figure 11(h–j)**. The results showed that the electrode generated a Nyquist diagram with the same shape as an ideal supercapacitor, demonstrating good contact between the rGO electrode and the copper electrode. In addition, Shen et al.[88] mixed sublimated sulfur and GO solution, which were brought into a concentrate, to prepare ink and formed a sulfur copolymer-graphene structure (3DP-pSG) with periodic micro-lattices by extrusion 3D printing, as shown in **Figure 11(a)**. It is found that the structure has a high reversible capacity of 812.8 $mA.h.g^{-1}$ and good cycle performance. Recently, researchers have found[89,90] that when the content of carbon nanomaterials in polymer composites is higher, carbon nanomaterials can form more compact microstructures and well-connected conductive networks with lower electrical resistance. The above research works provide some guidance for the application of 3D-printed carbon-based polymer composites in the field of energy storage.

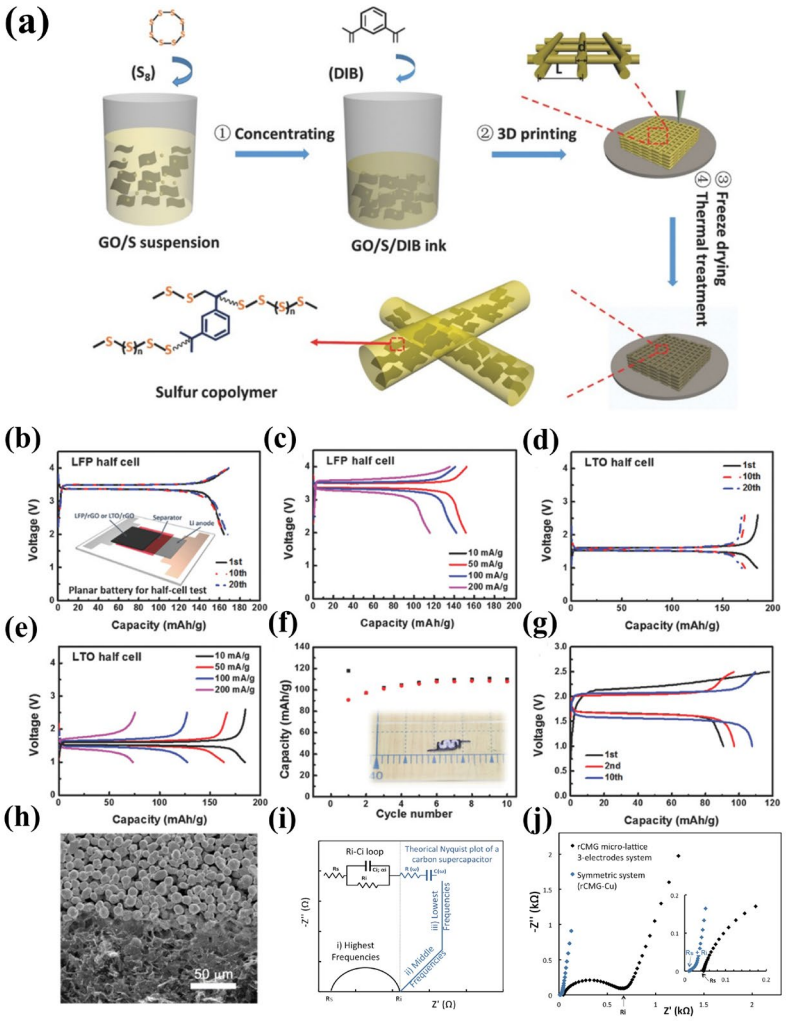

Figure 11. (a) Schematic demonstration of 3D printing sulfur copolymer-graphene (3DP-pSG) architectures. Aqueous GO suspension was homogeneously mixed with sublimed sulfur and concentrated into gel-like ink; then, 1,3-diisopropenylbenzene (DIB) was added to the ink and mixed homogeneously. As-prepared ink was placed into a 3 mL syringe and printed into layer-by-layer architectures. Afterward, the printed architectures were freeze-dried. Finally, sulfur copolymer was synthesized on the graphene nanowalls by thermal treatment at 200 °C[88]. **(b)** Charge and discharge profiles of LFP/rGO half-cell at specific current of 10 mA.g^{-1}. **(c)** Rate profiles of LFP/rGO half-cell at various specific currents. **(d)** Charge and discharge profiles of LTO/rGO half-cell at specific current of 10 mA.g^{-1}. **(e)** Rate profiles of LTO/rGO half-cell at various specific currents. **(f)** Cycling stability of 3D-printed full cell. The inset is a digital image of the 3D-printed full cell consisting of LFP/rGO, LTO/rGO, and polymer electrolyte. **(g)** Charge and discharge profiles of 3D-printed full cell[86]. **(h)** SEM images of reduced chemically modified graphene(rCMG)/Cu interface. **(i)** Typical Nyquist plot of carbon–carbon supercapacitor. It includes the high- to low-frequency behaviors of a supercapacitor with the equivalent circuits (R_s is high-frequency resistance, R_i is resistance of active material/current collector interface, C_i is interface capacitance with dispersion parameter α_i, R(ω) is part of supercapacitor resistance depending on frequency, and C(ω) is supercapacitor cell capacitance). **(j)** Nyquist plots recorded from 100 kHz to 10 mHz for three-electrode (blue) and symmetric (black) systems in EMI-TFSI electrolyte, with corresponding magnification of high- and mid-frequency responses[87].

The development of 3D printing to manufacture hydrogel structures has made it possible to mass-produce engineered cartilage tissues. Recently, Wang et al.[100] used NaOH solution to treat 3D-printed poly(ε-caprolactone) (PCL) scaffolds with low concentrations of graphene, as shown in **Figure 12(b)**. The results of the study showed that the scaffolds treated with NaOH were more biocompatible with cells. Cheng et al.[101] connected a 3D bioprinted microinjection system with a biopolymer reservoir, using chondrocytes to seed GO/chitosan hydrogels, as shown in **Figure 12(c,d)**. The results of the study showed that, compared with pure hydrogel, the 3D-printed GO/hydrogel tissue had thicker new cartilage after transplantation into cartilage tissue. In addition, Chen et al.[102] dissolved thermoplastic polyurethane (TPU) and graphene oxide (GO) in dimethylformamide (DMF) and polylactic acid (PLA) in dichloromethane (DCM), respectively, as shown in

Figure 12(a,g–j). Then, the mixture was precipitated and dried using an extruder to make a composite filament, which can be used directly in an FDM printer. The results of the study showed that the mechanical properties and thermal stability of the composites added with GO significantly improved, and the scaffolds showed good biocompatibility with NIH_3T_3 cells. Sayyar et al.[103] successfully prepared polytrimethylene carbonate (PTMC)/carbon nanomaterial composites by the extrusion deposition 3D printing method, as shown in **Figure 12(e,f)**. Through the comparison experiment before and after the addition of carbon nanomaterials, it was found that there was no significant difference in the DNA content of cells on the two scaffolds. This showed that the addition of carbon nanomaterials had no effect on the number of cells. Therefore, carbon-based polymer composites have important application prospects in the field of biomedical materials, especially in the development of new conductive scaffolds for tissue engineering.

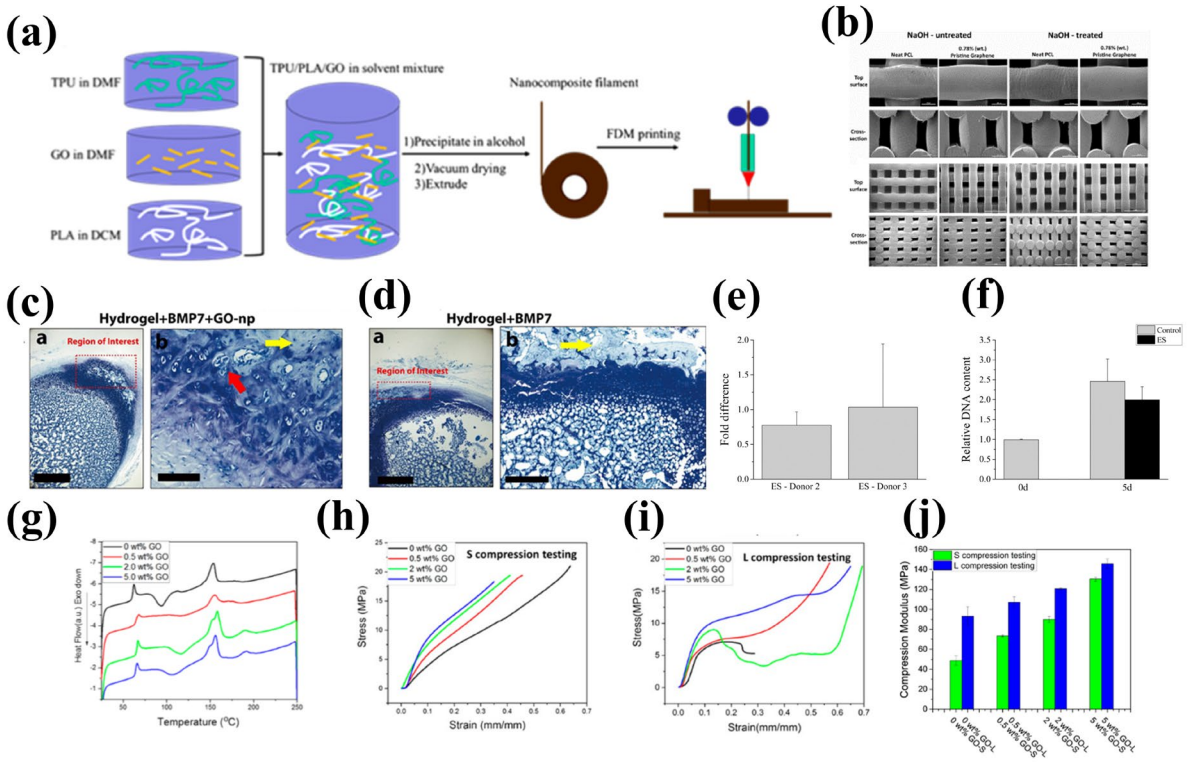

Figure 12. (a) TPU/PLA/GO nanocomposites filament preparation and FDM printing process[102]. **(b)** Top surface and cross-section scanning electron microscope images of neat PCL and 0.78wt% pristine graphene scaffolds treated and untreated with NaOH[100]. **(c)** Toluidine staining of hydrogel + BMP7 + GO-np transplanted in cartilage of rat knees. **(d)** Toluidine staining of hydrogel + BMP7 + transplanted in cartilage of rat knees. In the region of interest, the neogenetic cartilage of the hydrogel + BMP7 was thinner than hydrogel + BMP7 + GO-np (graphene oxide nanoparticles) (yellow arrow), and no neogenetic chondrocytes were observed in the hydrogel + BMP7 group (red arrow)[101]. **(e)** Effect of electrical stimulation (ES) on mesenchymal stem cell (MSC) numbers relative to unstimulated controls. Results are shown as a fold difference relative to the unstimulated control after five days of ES. **(f)** Cell number measured at two time points (donor 2)[103]. **(g)** Differential scanning calorimetry (DSC) curves of samples at different GO loadings. **(h)** S compression testing curves of samples of different GO loadings. **(i)** L compression testing curves of samples of different GO loadings. **(j)** Compression modulus of L and S compression testing of samples of different GO loadings[102].

5. Conclusion and perspective

Carbon-based polymer matrix composites and 3D printing are two research directions that have developed rapidly in recent years. Combining the two and taking advantage of their respective advantages can provide an effective solution for the complex structural molding of carbon-based polymer composites. Therefore, stretchable conductive nanocomposites prepared using carbon-based fillers provide a new research direction for next-generation electronic devices. However, the research and application of stretchable conductive polymer composites based on nanocarbon fillers are still in their infancy and still face many problems and

challenges. It mainly includes the following three aspects: (i) in the existing composite methods, the dispersion of carbon nanomaterials in the polymer carrier is poor, which results in the inability to fully utilize the excellent mechanical and electrical properties of carbon nanomaterials; (ii) problems, such as nozzle clogging and insufficient bonding force, are prone to occur during the 3D printing process, which greatly affects the performance of carbon-based polymer composite materials; and (iii) the types of polymers currently available for 3D printing are relatively limited, which requires further expansion.

Future research on stretchable conductive polymer composites based on nanocarbon fillers will mainly focus on the following aspects: (i) a suitable mixing method and certain chemical additives can be used to improve the dispersion of conductive fillers in the polymer, (ii) a variety of carbon nanomaterials can be used together to construct a stable and efficient conductive network, (iii) carbon nanomaterials have strong modification ability and can be modified according to specific applications, and (iv) miniaturization and large-scale fabrication of stretchable electronic devices can be achieved by developing novel printing techniques. Through the summary of the existing research, it is believed that stretchable conductive polymer composites prepared based on nano-carbon fillers can be used in many fields, such as stretchable electronic devices, which promotes the progress of related research fields.

Author contributions

CZ and RL contributed equally. CZ, RL, and RM proposed the topic of the work. HL, LW, YW, and RW were responsible for image beautification. BF, ZW, ZS, and RW revised the literature and provided the content. Correspondence should be addressed to RM. All authors have read and agreed to the published version of the manuscript.

Acknowledgments

This research was supported by the Shanghai pilot Program for Basic Research (grant no. 22TQ1400100-8), the Shanghai Pujiang Program (grant no. 20PJ1402500), the Natural Science Foundation of Shanghai (grant no. 22ZR1416600), and the Fundamental Research Funds for the Central Universities.

Conflict of interest

The authors declare no conflict of interest.

References

1. Cao D, Xing Y, Tantratian K, et al. 3D printed high-performance lithium metal microbatteries enabled by nanocellulose. *Advanced Materials* 2019; 31(14): 1807313. doi: 10.1002/adma.201807313
2. Chen X. Making electrodes stretchable. *Small Methods* 2017; 1(4): 1600029. doi: 10.1002/smtd.201600029
3. Lv Z, Li W, Yang L, et al. Custom-made electrochemical energy storage devices. *ACS Energy Letters* 2019; 4(2): 606–614. doi: 10.1021/acsenergylett.8b02408
4. Zhao C, Wang R, Fang B, et al. Boosting the lithium storage properties of a flexible $Li_4Ti_5O_{12}$/graphene fiber anode via a 3D printing assembly strategy. *Batteries* 2023; 9(10): 493. doi: 10.3390/batteries9100493
5. Wang C, Xia K, Wang H, et al. Advanced carbon for flexible and wearable electronics. *Advanced Materials* 2019; 31(9): 1801072. doi: 10.1002/adma.201801072
6. Bokobza L. Mechanical and electrical properties of elastomer nanocomposites based on different carbon nanomaterials. *C—Journal of Carbon Research* 2017; 3(2): 10. doi: 10.3390/c3020010
7. Mondal S, Khastgir D. Elastomer reinforcement by graphene nanoplatelets and synergistic improvements of electrical and mechanical properties of composites by hybrid nano fillers of graphene-carbon black & graphene-MWCNT. *Composites Part A: Applied Science and Manufacturing* 2017; 102: 154–165. doi: 10.1016/j.compositesa.2017.08.003
8. Ryan KR, Down MP, Hurst NJ, et al. Additive manufacturing (3D printing) of electrically conductive polymers and polymer nanocomposites and their applications. *eScience* 2022; 2(4): 365–381. doi: 10.1016/j.esci.2022.07.003

9. Huang A, Ma Y, Peng J, et al. Tailoring the structure of silicon-based materials for lithium-ion batteries via electrospinning technology. *eScience* 2021; 1(2): 141–162. doi: 10.1016/j.esci.2021.11.006
10. Wang Z, Gao W, Zhang Q, et al. 3D-printed graphene/polydimethylsiloxane composites for stretchable and strain-insensitive temperature sensors. *ACS Applied Materials & Interfaces* 2019; 11(1): 1344–1352. doi: 10.1021/acsami.8b16139
11. Mo R, Rooney D, Sun K, Yang HY. 3D nitrogen-doped graphene foam with encapsulated germanium/nitrogen-doped graphene yolk-shell nanoarchitecture for high-performance flexible Li-ion battery. *Nature Communications* 2017; 8(1): 13949. doi: 10.1038/ncomms13949
12. Zhao C, Liang H, Wang R, et al. Recent advances in high value-added carbon materials prepared from carbon dioxide for energy storage applications. *Carbon Capture Science & Technology* 2023; 9: 100144. doi: 10.1016/j.ccst.2023.100144
13. de Leon AC, Chen Q, Palaganas NB, et al. High performance polymer nanocomposites for additive manufacturing applications. *Reactive and Functional Polymers* 2016; 103: 141–155. doi: 10.1016/j.reactfunctpolym.2016.04.010
14. Song WJ, Lee S, Song G, Park S. Stretchable aqueous batteries: Progress and prospects. *ACS Energy Letters* 2019; 4(1): 177–186. doi: 10.1021/acsenergylett.8b02053
15. Song Z, Ma T, Tang R, et al. Origami lithium-ion batteries. *Nature Communications* 2014; 5(1): 3140. doi: 10.1038/ncomms4140
16. Bao Y, Zhang XY, Zhang X, et al. Free-standing and flexible limntio$_4$/carbon nanotube cathodes for high performance lithium ion batteries. *Journal of Power Sources* 2016; 321: 120–125. doi: 10.1016/j.jpowsour.2016.04.121
17. Fu KK, Cheng J, Li T, Hu L. Flexible batteries: From mechanics to devices. *ACS Energy Letters* 2016; 1(5): 1065–1079. doi: 10.1021/acsenergylett.6b00401
18. Bao Y, Hong G, Chen Y, et al. Customized kirigami electrodes for flexible and deformable lithium-ion batteries. *ACS Applied Materials & Interfaces* 2020; 12(1): 780–788. doi: 10.1021/acsami.9b18232
19. Storck JL, Ehrmann G, Uthoff J, Diestelhorst E. Investigating inexpensive polymeric 3D printed materials under extreme thermal conditions. *Materials Futures* 2022; 1(1): 015001. doi: 10.1088/2752-5724/ac4beb
20. de Castro Motta J, Qaderi S, Farina I, et al. Experimental characterization and mechanical modeling of additively manufactured TPU components of innovative seismic isolators. *Acta Mechanica* 2022. doi: 10.1007/s00707-022-03447-5
21. Buchanan C, Gardner L. Metal 3D printing in construction: A review of methods, research, applications, opportunities and challenges. *Engineering Structures* 2019; 180: 332–348. doi: 10.1016/j.engstruct.2018.11.045
22. Zhu C, Liu T, Qian F, et al. 3D printed functional nanomaterials for electrochemical energy storage. *Nano Today* 2017; 15: 107–120. doi: 10.1016/j.nantod.2017.06.007
23. Zhang F, Wei M, Viswanathan VV, et al. 3D printing technologies for electrochemical energy storage. *Nano Energy* 2017; 40: 418–431. doi: 10.1016/j.nanoen.2017.08.037
24. Sousa RE, Costa CM, Lanceros-Méndez S. Advances and future challenges in printed batteries. *ChemSusChem* 2015; 8(21): 3539–3555. doi: 10.1002/cssc.201500657
25. Tian X, Jin J, Yuan S, et al. Emerging 3D-printed electrochemical energy storage devices: A critical review. *Advanced Energy Materials* 2017; 7(17): 1700127. doi: 10.1002/aenm.201700127
26. Guo W, Wang X, Yang C, et al. Microfluidic 3D printing polyhydroxyalkanoates-based bionic skin for wound healing. *Materials Futures* 2022; 1: 015401. doi: 10.1088/2752-5724/ac446b
27. Park S, Shou W, Makatura L, et al. 3D printing of polymer composites: Materials, processes, and applications. *Matter* 2022; 5(1): 43–76. doi: 10.1016/j.matt.2021.10.018
28. de Leon AC, Rodier BJ, Bajamundi C, et al. Plastic metal-free electric motor by 3D printing of graphene-polyamide powder. *ACS Applied Energy Materials* 2018; 1(4): 1726–1733. doi: 10.1021/acsaem.8b00240
29. Hall A, Kong GX, Karanassios V. Detectors and light-sources for optical spectrometry: From a 3D-printed light-source to a self-powered sensor fabricated on a flexible polymeric substrate, and from there on to an IoT-enabled "smart" system. In: Proceedings of the 2019 IEEE International Conference on Flexible and Printable Sensors and Systems (FLEPS); 8–10 July 2019; Glasgow, UK. pp. 1–3. doi:10.1109/fleps.2019.8792321
30. Kurra N, Jiang Q, Nayak P, Alshareef HN. Laser-derived graphene: A three-dimensional printed graphene electrode and its emerging applications. *Nano Today* 2019; 24: 81–102. doi: 10.1016/j.nantod.2018.12.003
31. Li C, Cheng J, He Y, et al. Polyelectrolyte elastomer-based ionotronic sensors with multi-mode sensing capabilities via multi-material 3D printing. *Nature Communications* 2023; 14(1): 4853. doi: 10.1038/s41467-023-40583-5
32. Li K, Liang M, Wang H, et al. 3D mxene architectures for efficient energy storage and conversion. *Advanced Functional Materials* 2020; 30(47): 2000842. doi: 10.1002/adfm.202000842
33. Lyu Z, Lim GJH, Koh JJ, et al. Design and manufacture of 3D-printed batteries. *Joule* 2021; 5(1): 89–114. doi: 10.1016/j.joule.2020.11.010
34. Park J, Kim JK, Park SA, et al. 3D-printed biodegradable polymeric stent integrated with a battery-less pressure

sensor for biomedical applications. In: Proceedings of the 2017 19th International Conference on Solid-State Sensors, Actuators and Microsystems (TRANSDUCERS); 18–22 June 2017; Kaohsiung, Taiwan. pp. 14–50. doi: 10.1109/transducers.2017.7993984
35. Ngo TD, Kashani A, Imbalzano G, et al. Additive manufacturing (3D printing): A review of materials, methods, applications and challenges. *Composites Part B: Engineering* 2018; 143: 172–196. doi: 10.1016/j.compositesb.2018.02.012
36. Zhu Y, Murali S, Cai W, et al. Graphene and graphene oxide: Synthesis, properties, and applications. *Advanced Materials* 2010; 22(35): 3906–3024. doi: 10.1002/adma.201001068
37. Unwin PR, Güell AG, Zhang G. Nanoscale electrochemistry of sp^2 carbon materials: From graphite and graphene to carbon nanotubes. *Accounts of Chemical Research* 2016; 49(9): 2041–2408. doi: 10.1021/acs.accounts.6b00301
38. Smith M. New developments in carbon fiber. *Reinforced Plastics* 2018; 62(5): 266–269. doi: 10.1016/j.repl.2017.07.004
39. Fu X, Xu L, Li J, et al. Flexible solar cells based on carbon nanomaterials. *Carbon* 2018; 139: 1063–1073. doi: 10.1016/j.carbon.2018.08.017
40. Bhagavatheswaran ES, Parsekar M, Das A, et al. Construction of an interconnected nanostructured carbon black network: Development of highly stretchable and robust elastomeric conductors. *The Journal of Physical Chemistry C* 2015; 119(37): 21723–21731. doi: 10.1021/acs.jpcc.5b06629
41. Niu XZ, Peng SL, Liu LY, et al. Characterizing and patterning of PDMS-based conducting composites. *Advanced Materials* 2007; 19(18): 2682–2686. doi: 10.1002/adma.200602515
42. Song WJ, Park J, Kim DH, et al. Jabuticaba-inspired hybrid carbon filler/polymer electrode for use in highly stretchable aqueous Li-ion batteries. *Advanced Energy Materials* 2018; 8(10): 1702478. doi: 10.1002/aenm.201702478
43. Shin MK, Oh J, Lima M, et al. Elastomeric conductive composites based on carbon nanotube forests. *Advanced Materials* 2010; 22(24): 2663–2667. doi: 10.1002/adma.200904270
44. Sekitani T, Nakajima H, Maeda H, et al. Stretchable active-matrix organic light-emitting diode display using printable elastic conductors. *Nature Materials* 2009; 8(6): 494–499. doi: 10.1038/nmat2459
45. Liu Z, Qian Z, Song J, Zhang Y. Conducting and stretchable composites using sandwiched graphene-carbon nanotube hybrids and styrene-butadiene rubber. *Carbon* 2019; 149: 181–189. doi: 10.1016/j.carbon.2019.04.037
46. Gao N, Fang X. Synthesis and development of graphene—Inorganic semiconductor nanocomposites. *Chemical Reviews* 2015; 115(16): 8294–83343. doi: 10.1021/cr400607y
47. Chen Z, Ren W, Gao L, et al. Three-dimensional flexible and conductive interconnected graphene networks grown by chemical vapour deposition. *Nature Materials* 2011; 10(6): 424–428. doi: 10.1038/nmat3001
48. Wang Z, Liu X, Shen X, et al. An ultralight graphene honeycomb sandwich for stretchable light-emitting displays. *Advanced Functional Materials* 2018; 28(19): 1707043. doi: 10.1002/adfm.201707043
49. Sun F, Tian M, Sun X, et al. Stretchable conductive fibers of ultrahigh tensile strain and stable conductance enabled by a worm-shaped graphene microlayer. *Nano Letters* 2019; 19(9): 6592–6599. doi: 10.1021/acs.nanolett.9b02862
50. Praveena BA, Lokesh N, Buradi A, et al. A comprehensive review of emerging additive manufacturing (3D printing technology): Methods, materials, applications, challenges, trends and future potential. *Materials Today: Proceedings* 2022; 52(Part 3): 1309–1313. doi: 10.1016/J.MATPR.2021.11.059
51. Kristiawan RB, Imaduddin F, Ariawan D, et al. A review on the fused deposition modeling (FDM) 3D printing: Filament processing, materials, and printing parameters. *Open Engineering* 2021; 11(1): 639–649. doi: 10.1515/ENG-2021-0063
52. Pervaiz S, Qureshi TA, Kashwani G, Kannan S. 3D printing of fiber-reinforced plastic composites using fused deposition modeling: A status review. *Materials* 2021; 14(16): 4520. doi: 10.3390/MA14164520
53. Wei X, Li D, Jiang W, et al. 3D printable graphene composite. *Scientific Reports* 2015; 5(1): 11181. doi: 10.1038/srep11181
54. Zhu D, Ren Y, Liao G, et al. Thermal and mechanical properties of polyamide 12/graphene nanoplatelets nanocomposites and parts fabricated by fused deposition modeling. *Journal of Applied Polymer Science* 2017; 134(39): 45332. doi: 10.1002/app.45332
55. Saadi MASR, Maguire A, Pottackal NT, et al. Direct ink writing: A 3D printing technology for diverse materials. *Advanced Materials* 2022; 34(28): 2108855. doi: 10.1002/ADMA.202108855
56. Singh M, Haverinen HM, Dhagat P, Jabbour GE. Inkjet printing—Process and its applications. *Advanced Materials* 2010; 22(6): 673–685. doi: 10.1002/adma.200901141
57. Lim S, Kang B, Kwak D, et al. Inkjet-printed reduced graphene oxide/poly(vinyl alcohol) composite electrodes for flexible transparent organic field-effect transistors. *The Journal of Physical Chemistry C* 2012; 116(13): 7520–7525. doi: 10.1021/jp203441e
58. García-Tuñon E, Barg S, Franco J, et al. Printing in three dimensions with graphene. *Advanced Materials* 2015; 27(10): 1688–1693. doi: 10.1002/adma.201405046

59. Uçak N, Çiçek A, Aslantas K. Machinability of 3D printed metallic materials fabricated by selective laser melting and electron beam melting: A review. *Journal of Manufacturing Processes* 2022; 80: 414–457. doi: 10.1016/J.JMAPRO.2022.06.023
60. Acord KA, Dupuy AD, Scipioni Bertoli U, et al. Morphology, microstructure, and phase states in selective laser sintered lithium ion battery cathodes. *Journal of Materials Processing Technology* 2021; 288: 116827. doi: 10.1016/J.JMATPROTEC.2020.116827
61. Zhou X, Nowicki M, Cui H, et al. 3D bioprinted graphene oxide-incorporated matrix for promoting chondrogenic differentiation of human bone marrow mesenchymal stem cells. *Carbon* 2017; 116: 615–624. doi: 10.1016/j.carbon.2017.02.049
62. Pagac M, Hajnys J, Ma QP, et al. A review of vat photopolymerization technology: Materials, applications, challenges, and future trends of 3D printing. *Polymers* 2021; 13(4): 598. doi: 10.3390/POLYM13040598
63. Costa BMDC, Griveau S, Bedioui F, et al. Stereolithography based 3D-printed microfluidic device with integrated electrochemical detection. *Electrochimica Acta* 2022; 407: 139888. doi: 10.1016/J.ELECTACTA.2022.139888
64. Li C, Du J, Gao Y, et al. Stereolithography of 3D sustainable metal electrodes towards high-performance nickel iron battery. *Advanced Functional Materials* 2022; 32(40): 2205317. doi: 10.1002/ADFM.202205317
65. Gaikwad S, Tate JS, Theodoropoulou N, Koo JH. Electrical and mechanical properties of PA11 blended with nanographene platelets using industrial twin-screw extruder for selective laser sintering. *Journal of Composite Materials* 2013; 47(23): 2973–2986. doi: 10.1177/0021998312460560
66. Shuai C, Feng P, Gao C, et al. Graphene oxide reinforced poly(vinyl alcohol): Nanocomposite scaffolds for tissue engineering applications. *RSC Advances* 2015; 5: 25416–25423. doi: 10.1039/C4RA16702C
67. Zhai F, Feng Y, Li Z, et al. 4D-printed untethered self-propelling soft robot with tactile perception: Rolling, racing, and exploring. *Matter* 2021; 4(10): 3313–3326. doi: 10.1016/J.MATT.2021.08.014
68. Yu Y, Feng Y, Liu F, et al. Carbon dots-based ultrastretchable and conductive hydrogels for high-performance tactile sensors and self-powered electronic skin. *Small* 2023; 19(31): 2204365. doi: 10.1002/SMLL.202204365
69. Zhu Y, Tang T, Zhao S, et al. Recent advancements and applications in 3D printing of functional optics. *Additive Manufacturing* 2022; 52: 102682. doi: 10.1016/J.ADDMA.2022.102682
70. Jiang Y, Islam MN, He R, et al. Recent advances in 3D printed sensors: Materials, design, and manufacturing. *Advanced Materials Technologies* 2023; 8(2): 2200492. doi: 10.1002/ADMT.202200492
71. Tan HW, Choong YYC, Kuo CN, et al. 3D printed electronics: Processes, materials and future trends. *Progress in Materials Science* 2022; 127: 100945. doi: 10.1016/J.PMATSCI.2022.100945
72. Zhang F, Feng Y, Feng W. Three-dimensional interconnected networks for thermally conductive polymer composites: Design, preparation, properties, and mechanisms. *Materials Science and Engineering: R: Reports* 2020; 142: 100580. doi: 10.1016/J.MSER.2020.100580
73. Li Z, Wang L, Li Y, et al. Carbon-based functional nanomaterials: Preparation, properties and applications. *Composites Science and Technology* 2019; 179: 10–40. doi: 10.1016/J.COMPSCITECH.2019.04.028
74. Zhang D, Chi B, Li B, et al. Fabrication of highly conductive graphene flexible circuits by 3D printing. *Synthetic Metals* 2016; 217: 79–86. doi: 10.1016/j.synthmet.2016.03.014
75. Liu H, Zhang H, Han W, et al. 3D printed flexible strain sensors: From printing to devices and signals. *Advanced Materials* 2021; 33(8): 2004782. doi: 10.1002/ADMA.202004782
76. Schwierz F. Graphene transistors. *Nature Nanotechnology* 2010;5(7): 487–496. doi: 10.1038/nnano.2010.89
77. Xiang L, Wang Z, Liu Z, et al. Inkjet-printed flexible biosensor based on graphene field effect transistor. *IEEE Sensors Journal* 2016; 16(23): 8359–8364. doi: 10.1109/JSEN.2016.2608719
78. Huang L, Huang Y, Liang J, et al. Graphene-based conducting inks for direct inkjet printing of flexible conductive patterns and their applications in electric circuits and chemical sensors. *Nano Research* 2011; 4(7): 675–684. doi: 10.1007/s12274-011-0123-z
79. Willian MD, Michaela E, Mae CH, et al. A comprehensive review on the application of 3D printing in the aerospace industry. *Key Engineering Materials* 2022; 913: 27–34. doi: 10.4028/p-94a9zb
80. Mohanavel V, Ashraff Ali KS, Ranganathan K, et al. The roles and applications of additive manufacturing in the aerospace and automobile sector. *Materials Today: Proceedings* 2021; 47: 405–409. doi: 10.1016/J.MATPR.2021.04.596
81. Sugiyama K, Matsuzaki R, Ueda M, et al. 3D printing of composite sandwich structures using continuous carbon fiber and fiber tension. *Composites Part A: Applied Science and Manufacturing* 2018; 113: 114–121. doi: 10.1016/J.COMPOSITESA.2018.07.029
82. Sai Saran O, Prudhvidhar Reddy A, Chaturya L, Pavan Kumar M. 3D printing of composite materials: A short review. *Materials Today: Proceedings* 2022; 64: 615–619. doi: 10.1016/J.MATPR.2022.05.144
83. Wang X, Jin J, Song M. An investigation of the mechanism of graphene toughening epoxy. *Carbon* 2013; 65: 324–333. doi: 10.1016/j.carbon.2013.08.032
84. Verma M, Verma P, Dhawan SK, Choudhary V. Tailored graphene based polyurethane composites for efficient electrostatic dissipation and electromagnetic interference shielding applications. *RSC Advances* 2015; 5(118):

97349–97358. doi: 10.1039/C5RA17276D
85. Singh AP, Garg P, Alam F, et al. Phenolic resin-based composite sheets filled with mixtures of reduced graphene oxide, γ-Fe_2O_3 and carbon fibers for excellent electromagnetic interference shielding in the X-band. *Carbon* 2012; 50(10): 3868–3875. doi: 10.1016/j.carbon.2012.04.030
86. Fu K, Wang Y, Yan C, et al. Graphene oxide-based electrode inks for 3D-printed lithium-ion batteries. *Advanced Materials* 2016; 28(13): 2587–2594. doi: 10.1002/adma.201505391
87. Rocha VG, García-Tuñón E, Botas C, et al. Multimaterial 3D printing of graphene-based electrodes for electrochemical energy storage using thermoresponsive inks. *ACS Applied Materials &Interfaces* 2017; 9(42): 37136–37145. doi: 10.1021/acsami.7b10285
88. Shen K, Mei H, Li B, et al. 3D printing sulfur copolymer-graphene architectures for Li-S batteries. *Advanced Energy Materials* 2018; 8(4): 1701527. doi: 10.1002/aenm.201701527
89. Huang K, Yang J, Dong S, et al. Anisotropy of graphene scaffolds assembled by three-dimensional printing. *Carbon* 2018; 130: 1–10. doi: 10.1016/j.carbon.2017.12.120
90. Vernardou D, Vasilopoulos KC, Kenanakis G. 3D printed graphene-based electrodes with high electrochemical performance. *Applied Physics A* 2017; 123: 623. doi: 10.1007/s00339-017-1238-1
91. Fan D, Li Y, Wang X, et al. Progressive 3D printing technology and its application in medical materials. *Frontiers in Pharmacology* 2020; 11: 516624. doi: 10.3389/FPHAR.2020.00122/BIBTEX
92. Al-Dulimi Z, Wallis M, Tan DK, et al. 3D printing technology as innovative solutions for biomedical applications. *Drug Discovery Today* 2021; 26(2): 360–383. doi: 10.1016/J.DRUDIS.2020.11.013
93. Chadha U, Abrol A, Vora NP, et al. Performance evaluation of 3D printing technologies: A review, recent advances, current challenges, and future directions. *Progress in Additive Manufacturing* 2022; 7(5): 853–886. doi: 10.1007/S40964-021-00257-4
94. Mallakpour S, Tabesh F, Hussain CM. 3D and 4D printing: From innovation to evolution. *Advances in Colloid and Interface Science* 2021; 294: 102482. doi: 10.1016/J.CIS.2021.102482
95. Zhang L, Forgham H, Shen A, et al. Nanomaterial integrated 3D printing for biomedical applications. *Journal of Materials Chemistry B* 2022; 10(37): 7473–7490. doi: 10.1039/D2TB00931E
96. Kantaros A. 3D printing in regenerative medicine: Technologies and resources utilized. *International Journal of Molecular Sciences* 2022; 23(23): 14621. doi: 10.3390/IJMS232314621
97. Pavan Kalyan BG, Kumar L. 3D printing: Applications in tissue engineering, medical devices, and drug delivery. *AAPS PharmSciTech* 2022; 23(4): 1–20. doi: 10.1208/S12249-022-02242-8
98. Kalkal A, Kumar S, Kumar P, et al. Recent advances in 3D printing technologies for wearable (bio)sensors. *Additive Manufacturing* 2021; 46: 102088. doi: 10.1016/J.ADDMA.2021.102088
99. Bozkurt Y, Karayel E. 3D printing technology; methods, biomedical applications, future opportunities and trends. *Journal of Materials Research and Technology* 2021; 14: 1430–1450. doi: 10.1016/J.JMRT.2021.07.050
100. Wang W, Caetano G, Ambler WS, et al. Enhancing the hydrophilicity and cell attachment of 3D printed PCL/graphene scaffolds for bone tissue engineering. *Materials (Basel)* 2016; 9(12): 992. doi: 10.3390/ma9120992
101. Cheng Z, Landish B, Chi Z, et al. 3D printing hydrogel with graphene oxide is functional in cartilage protection by influencing the signal pathway of Rank/Rankl/OPG. *Materials Science and Engineering: C* 2018; 82: 244–252. doi: 10.1016/j.msec.2017.08.069
102. Chen Q, Mangadlao JD, Wallat J, et al. 3D printing biocompatible polyurethane/poly(lactic acid)/graphene oxide nanocomposites: Anisotropic properties. *ACS Applied Materials & Interfaces* 2017; 9(4): 4015–4023. doi: 10.1021/acsami.6b11793
103. Sayyar S, Bjorninen M, Haimi S, et al. UV cross-linkable graphene/poly(trimethylene carbonate) composites for 3D printing of electrically conductive scaffolds. *ACS Applied Materials & Interfaces* 2016; 8(46): 31916–31925. doi: 10.1021/acsami.6b09962